A 3D segmentation framework for an accurate extraction of the spongy and cortical bones from the MRI data

Seyed Mehdi Moghadas, Won-Sook Lee
School of Electrical Engineering and Computer Science
University of Ottawa
Ottawa, ON, Canada
Smogh098@uottawa.ca

***Abstract*— In this paper we proposed a new framework for obtaining the spongy and cortical bones from the MRI data. The method focuses on the accurate extraction of the edges of the target tissues, which is the main drawback of the previous works. This framework first limits the searching area for the bone voxels from the whole data to a small strip around the edges of the cortical and spongy bones then applies a very accurate segmentation on the searching area using the newly developed deformable kernel Fuzzy C-Means (DKFCM) algorithm, which is proposed in this paper. Comparing the results of this work with previous segmentation methods on a testing dataset consisting of 10,485,760 voxels demonstrates the superiority of the proposed method especially on the edges of the spongy and cortical bone.**

Keywords—MRI; Segmentation; Fuzzy C-Means; Spongy bone; Cortical bone;

I. INTRODUCTION

Magnetic resonance imaging (MRI) is currently a useful method for exploring the body organs. MRI gives us a 3D image of the body's internal organs, which can be used for 3D modeling of the organs after segmentation. 3D modeling of the organs has various applications like surgery assistance [14], diagnosing the cartilage degradation [7, 11] and diagnosing the musculoskeletal disorders in a specific patient [2] like the Femoroacetabular impingement (FAI) [21].

Segmenting the MRI data and extracting the target tissue is the first step for exploiting the MRI data. Manual segmentation of the MRI is very time consuming and expensive for one patient. On the other hand due to the inherent noise and intensity overlapping, automatic segmentation of the MRI data is a challenging issue. Robustness against the noise, correct detection of the tissues and accurate segmentation of the edges of each tissue are the most challenging tasks for any MRI segmentation method.

The goal of this work is developing a new framework to extract the cortical and spongy bone very accurately from the MRI data with minimal interaction from the human. The results of this work can be used in the modeling of bones in a specific patient for detecting the skeletal disorders and structural analysis of the cortical and spongy bones in patients[20]. For this purpose, we proposed a framework that limits the segmentation area from the whole slice to a strip around the contour of the bone. As a result, most of the non-bone pixels which have overlap with the bone pixels are omitted. For increasing the segmentation accuracy on the edges of the bone, we proposed the DKFCM method. In this method by deforming a 3 dimensional kernel around the main pixel, which specifies the neighboring pixels, in an iterative mode the quality of the segmentation on the edges is improved.

The paper is organized in five sections. In section 2 we explore the previous works and their ability for segmenting the bone tissues. In section 3 the proposed method is explained. Section 4 explains the results of comparing the proposed method with previous works and section 5 is the conclusion.

II. RELATED WORKS

So far some different methods have been utilized for segmenting the MRI data. Deformable models [6, 8, 19], Markov Random Field [17, 1], graph cut [12], neural network [9, 10] and Fuzzy C-Means (FCM) [5, 13, 15] are some of these methods. However, there are few methods which are designed specifically for segmenting the bone. To address this problem, H. Kang et al. [3] proposed a framework for considering the expert knowledge about the placement of different tissues in segmenting the MRI of thigh to muscle, adipose tissue, spongy bone and cortical bone. Implementing this method and testing it with our dataset at section 4 for extracting the cortical and spongy bones showed that although this method could correct many of the miss-segmented parts in comparison with the segmentation by the FCM but the results still contain some miss-classified parts of the other tissues and the result of the segmentation on the edges is not accurate.

Benjamin Gilles et al. [6] made use of simplex meshes discrete model for musculoskeletal MRI segmentation. This method doesn't have the miss-classification problem on the main body of the tissues but it is still not accurate on the edges and it can't separate the cortical bone from the spongy bone.

FCM is another clustering method, which was proposed by J. C. Bezdek [16] and proves to be efficient in image segmentation. FCM works with updating the center of each cluster and membership function in an iterative process. Center

This work is supported by the Canadian Institutes of Health Research (CIHR) and the Natural Sciences and Engineering Research Council of Canada (NSERC)

of each cluster, v_i, is the central value of the cluster i and the membership function, w_{ik}, is the degree of membership of the pixel k to cluster i. The iteration ends when the change in the membership function in two successive iterations is less than a pre-specified number. The main drawback of this method is that it only considers the intensity of the pixels for clustering them. To address this deficiency, some methods [4, 5, 18] added the spatial information to the objective function of the FCM. So, the cluster of each pixel is decided based on the main pixel and the neighboring pixels around it. This extension of FCM, which is known as spatial FCM or SFCM, improves the robustness of the FCM against the noise however it doesn't improve the segmentation result on the edges of the tissues. The other problem is the miss-classification of some parts on the main body of one tissue as another tissue because of the intensity overlapping between the pixels in different tissues. In our method the miss-classification problem on the main body of tissues is resolved and the result of segmentation on the edges is improved.

III. THE FRAMEWORK FOR OBTAINING THE SPONGY AND CORTICAL BONE

A. *Selecting the bone parts at the seed slice*

The segmentation process begins from the seed slice and continues until the segmentation of whole of the slices. The seed slice can be selected from any of the slices in the Sagittal, Axial or Coronal views that contain a part of each of the bones in the MRI data. If a slice with all of the bone parts doesn't exist, we need to choose more than one seed slice to have all of the bone parts. The program can choose the seed slices based on the expert knowledge from the body regions.

The block diagram of the segmentation at the seed slice is shown in Fig. 1. The very first step is separating the bones from the other tissues. This is not an accurate segmentation we just need to have separate islands. A two dimensional slice of the hip joint is shown in Fig. 2 (a), as it's shown the spongy tissue is bonded with the cortical bone. Due to the lower intensity of the cortical bone in comparison with the spongy, muscle and adipose tissues, it's possible to isolate the spongy bone from other tissues, using gradient. For this purpose, first we apply canny edge detection on the seed slice to detect the connected edges and then deducting them from the slice. After deducting the edges for increasing the robustness of the framework to the noise, (noise can pierce through some parts of the edges and connect the spongy bone to some pixels of the muscle or adipose tissue) the GSFCM method [4] is utilized for detecting the spongy bones and making the ultimate pre-segmented image. The result of the pre-segmented image is shown in Fig. 2 (b). Next step is a very small interaction from the operator. For this purpose the pre-segmented image is provided to the operator and the operator should click on the bone parts. This interaction, at the worse condition doesn't take more than 5 seconds. Fig. 2 (c) shows the places of clicks by the operator. As we will explain at the part c of this section, clicking on the bone parts on the seed slice is enough for segmenting whole of the successive slices and the operator doesn't need to do anything on the other slices.

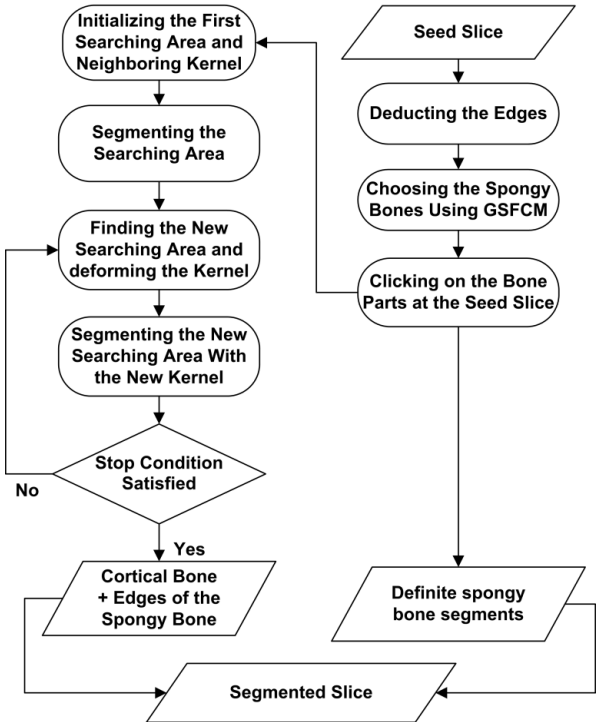

Fig. 1. The block diagram of the segmentation process at the seed slice

B. *Proposed deformable Kernel Fuzzy C-Means*

For an accurate segmentation of the tissues on the edges the newly developed DKFCM method is proposed in this paper. The core of this method is a generalized spatial FCM method. As it's explained in section 2, at the spatial FCM the cluster of each pixel is determined based on the main pixel and it's neighboring pixels. In DKFCM the neighboring voxels are

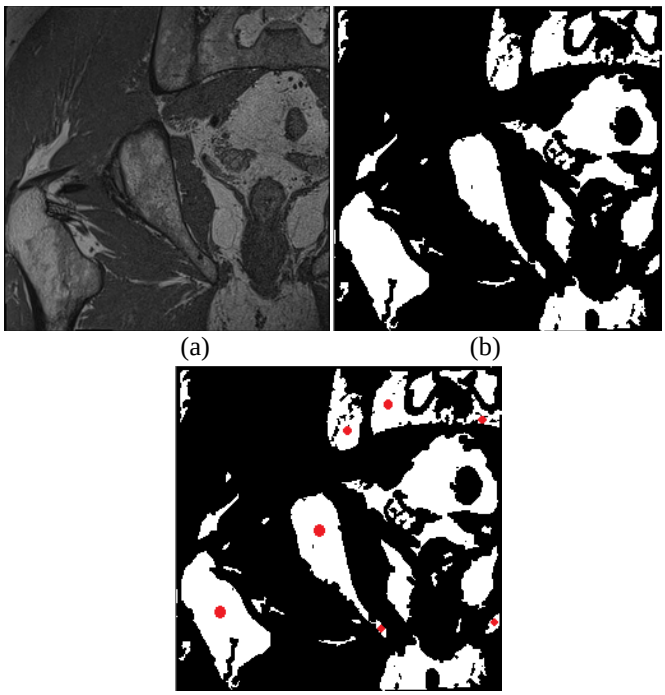

Fig. 2. (a) The original slice, (b) The pre-segmented slice provided to the operator, (c) places of clicks by the operator

bounded in a 3 dimensional deformable kernel around the main voxel. The method begins with initializing the first searching area and neighboring kernel at the block diagram of Fig. 1, continues by deforming the neighboring kernel and adjusting the searching area in an iterative mode based on the segmentation obtained at the previous iteration and ends when the result of segmentation converges and satisfies the stop condition.

As explained, the first step is initializing the searching area and the neighboring kernel. The initialized kernel is a 3×3×3 cube as shown in Fig. 3 (a). The initialized searching area is a strip around the chosen bone parts on the current, the next and the previous slices. The width of this strip is equal to the maximum width of the cortical bone at the MRI dataset plus five. After initialization, the searching area is segmented with the GSFCM method using the initialized neighboring kernel. GSFCM, which is proposed by Huynh Van Lung et al. [4], is a generalized version of the spatial FCM. This method considers the cluster of the neighboring pixels in addition to their distance from the central pixel. For this purpose, the function P_{ik} is defined as follows

$$P_{ik} = \sum_{j=0}^{N_k} g(u_{ij}) \left(\sum_{l=0}^{N_k} \frac{d^2(x_k, x_j)}{d^2(x_k, x_l)} \right)^{-1} \quad (1)$$

Where, N_k is the set of the neighborhood pixels around the central pixel k, which in our method we confine it to our deformable 3D kernel, u_{ij} is the membership value of the neighboring pixel j to cluster i and d() shows the distance between the pixels. Function P_{ik} is then used to calculate the membership function (w_{ik}) and the center of cluster (v_i) as follows. The clustering happens by updating the v_i and w_{ik} in an iterative process same as the process which is explained for FCM in section 2.

$$w_{ik} = \left[\frac{(d^2(x_k, v_i) f(P_{ik}))^{\frac{1}{m-1}}}{\sum_{j=1}^{c} (d^2(x_k, v_j) f(P_{jk}))^{\frac{1}{m-1}}} \right]^{-1} \quad (2)$$

$$v_i = \frac{\sum_{k=1}^{n} {w_{ik}}^m x_k}{\sum_{k=1}^{n} {w_{ik}}^m} \quad (3)$$

After segmenting the searching area with the initialized searching area and kernel and obtaining the cortical and spongy bone an iterative process begins for minimizing the segmentation error on the edges of the bone. At each of the iterations we change the searching area and the kernel in 3 dimensions, based on the obtained contour of the bone at the previous iteration and then, repeat the segmentation process. The iteration continues until the stop condition is fulfilled. Equations 4 and 5 show the stop condition.

$$\sum_{n \epsilon N_r} d\left(SI_n^{(r)} - SI_n^{(r-1)}\right) < \varepsilon_L \quad (4)$$

$$d\left(SI_n^{(r)} - SI_n^{(r-1)}\right) = \begin{cases} 1 & SI_n^{(r)} - SI_n^{(r-1)} \neq 0 \\ 0 & SI_n^{(r)} - SI_n^{(r-1)} = 0 \end{cases} \quad (5)$$

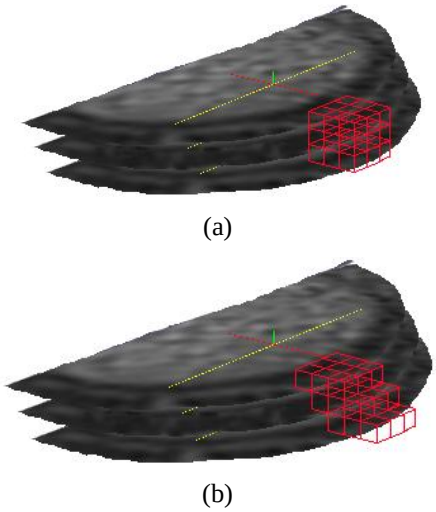

(a)

(b)

Fig. 3. (a) The deformable kernel at the first iteration, (b), The deformed kernel at the second iteration

Where, N_r is the set of searching area pixels at the current iteration. SI is the segmented searching area, r shows the current iteration and r-1 shows the last iteration. ε_L is a natural number defined by the user.

Fig. 3 shows the reforming process of the kernel Fig. 3 (a) shows the kernel at the first segmentation iteration and Fig. 3 (b) shows the kernel at the second iteration. The kernel is reformed to adapt itself with the position of the cortical bone in the current, next and previous slices.

The kernel is made of three movable blocks and the new distance between the position of the middle and top blocks and also the middle and bottom blocks in x and y coordinates are calculated by (6) and (7) respectively.

$$d_{ij}^{x} = \sum_{y=-1}^{1} B_y [(f_{jy} + l_{jy}) - (f_{iy} + l_{iy})] \quad (6)$$

$$d_{ij}^{y} = \sum_{x=-1}^{1} B_x [(f_{jx} + l_{jx}) - (f_{ix} + l_{ix})] \quad (7)$$

d_{ij} is the distance between the blocks at layers i and j. y is the row number in the block. For the main voxel the row number is zero for the voxels located under and above the main voxel the row number is assumed -1 and +1 respectively. B_y is the weight of each row. F_{iy} and l_{iy} are the first and last voxels of the cortical bone, which are located at the row y of the layer i.

For changing the searching area we simply considered the width of the cortical bone at the previous iteration. The new searching area is from the (width/2) pixels inside the cortical bone to (width/2) pixels outside it.

C. Back and forward propagation of the searching area

After the convergence of the algorithm in one slice and finding the spongy and cortical bone regions, an automatic back and forward propagation for finding the bone regions in the back and forward slices begins. The idea is that, because of the small distance between the slices, there is not a big change in the contour of the bone in successive slices. So having the

boundaries of the bone in one slice will help us to narrow - down our searching area for the bone in the back and forward slices from the whole image to just a strip around the current contour of the bone. In Fig. 4 a part of the bone at the current slice is marked, the definite spongy bone area at the next slice is bounded with the blue dashed line and the searching area at the next slice is the area between the red and blue dashed lines. In our dataset, which consists of 160 slices in the coronal view, the initialized searching area at the next slice is defined as 3 pixels outside the current contour of the bone and 3 pixels plus the width of the cortical bone inside it. After finding the definite spongy bone area and the initialized searching area at the next slice the process continues by applying DKFCM on the searching area of the next slice. The segmentation process continues until the segmentation of the last slice.

IV. EXPERIMENTAL RESULT

Because of the high rate of noise and intensity overlapping, neither the FCM nor the GSFCM have acceptable segmentation results on our dataset (the accuracy of the FCM and GSFCM are both less than 70%). So, we decided to implement the method proposed by H. Kang et al. [3] and compare its results with our method. This method provides a framework for segmenting the MRI data of thigh to spongy bone, cortical bone, muscle and fat using the expert knowledge about the relative position of the tissues and FCM together. Because of the proven superiority of the GSFCM to FCM, we implemented this method with FCM (as it was proposed originally in the paper) and with GSFCM. The segmentation results of two different slices using the method proposed in [3], the method proposed by [3] improved with GSFCM and the proposed method are shown in Fig. 5. For comparing the results of the proposed method and the method proposed by [3] on the edges two close views from the extracted spongy bone at the femur's head and acetabulum meeting point is shown in Fig. 6. The edges of the femur's head, acetabulum and the acetabular notch are clear in Fig. 6 (b). The results clearly show the superiority of the proposed method.

For the evaluation purposes, a testing dataset of 256×256×160 MRI data of hip joint (10,485,760 voxels) is prepared and the results of segmentation are compared with the ground truth. The accuracy is defined as the ratio of the number of truly segmented voxels of a specific tissue to the total number of the voxels of that tissue. The performance comparison results are shown in table I.

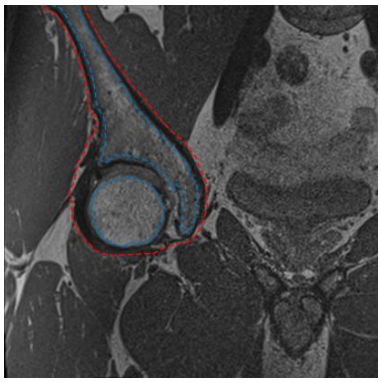

Fig. 4. The definite spongy bone and the searching areas

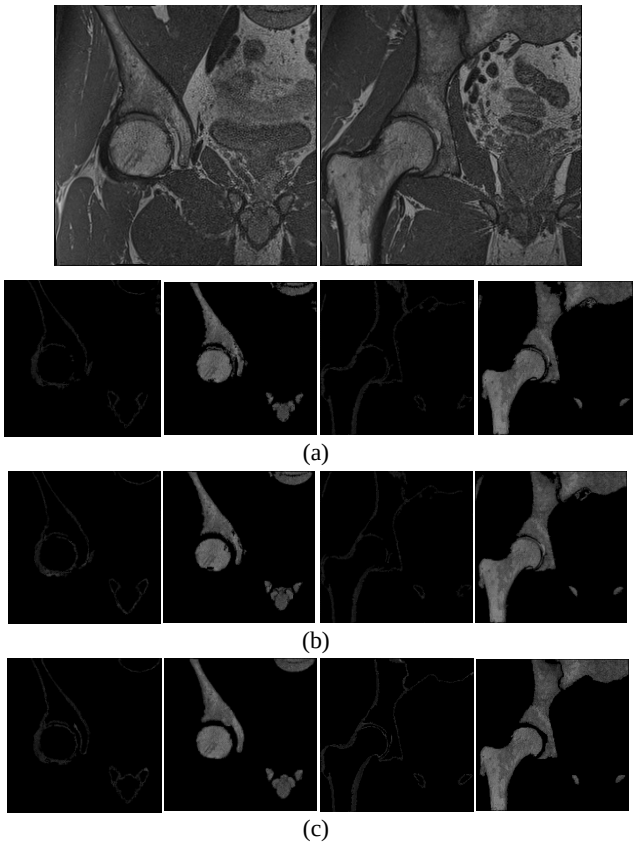

Fig. 5. The results of segmentation on two slices (a) Ref [3], (b) Ref [3] improved by GSFCM, (c) The proposed framework

The results show the superiority of the proposed method in any case. However the proposed method has better result on the edges in comparison with the overall result. This is very important because the good extraction of the edges is an important factor in MRI segmentation and most of the available segmentation methods have problem with this issue.

For a better evaluation, the false positive and negative are also calculated on the edges. As it's shown in table II, the false positive and negative are almost equal for the proposed method while for the method proposed by [3] the false positive is very bigger, which indicates that there are some parts of the other tissues, which are segmented as the bone. This proves the superiority of the proposed method in this case which is resulted from the accurate bounding of the searching area to the edges of the bone at the proposed framework.

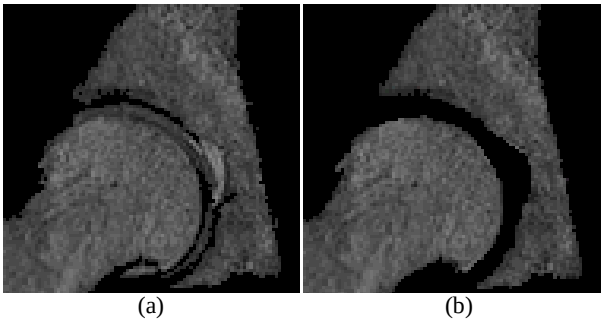

Fig. 6. Extracted spongy bone at the femur head and acetabulum meeting point by (a) Ref [3] improved by GSFCM, (b) The proposed framework

TABLE I. COMPARING THE ACCURACY OF SEGMENTATION IN THE PROPOSED FRAMEWORK WITH REF[3] AND REF [3] IMPROVED WITH THE GSFCM

Region	Ref [3]	Ref [3] with GSFCM	Proposed Method
Spongy and Cortical	83.1%	86.7%	97.2%
Spongy Bone	90.2%	92.9%	99.3%
Cortical Bone	67.8%	72.3%	90.4%
Edges (Spongy +cortical)	70.4%	73.1%	92.3%

TABLE II. COMPARING THE FALSE POSITIVE AND FALSE NEGATIVE IN THE PROPOSED FRAMEWORK WITH REF[3] AND REF [3] IMPROVED WITH THE GSFCM

Region and Error	Ref [3]	Ref [3] with GSFCM	Proposed Method
Edges (FP)	19.4%	18.2%	3.6%
Edges(FN)	10.2%	8.7%	4.1%

V. CONCLUSION

A new framework for obtaining the bone from the MRI data and segmenting it to the spongy and cortical bone is proposed. The DKFCM method, which is proposed in this paper and used in the framework, resulted to an accurate segmentation of the bone and demonstrates superiority over the previous works especially on the edges, which is the main shortcoming of the existing methods. The accuracy of this method on the edges demonstrates the potential of this method for obtaining the other tissues of the body like the muscle and adipose tissues from the MRI data, which can be considered in future works.

REFERENCES

[1] Ahmed B. Ashraf, Sara C. Gavenonis, Dania Daye, Carolyn Mies, Mark A. Rosen and Despina Kontos, "A Multichannel Markov Random Field Framework for Tumor Segmentation With an Application to Classification of Gene Expression-Based Breast Cancer Recurrence Risk", IEEE Transactions on Medical Imaging, vol. 32, no. 4, April 2013.

[2] Blemker S. Asakawa, D. Asakawa, G. Gold, S. Delp,"Image-based musculoskefletal modeling: applications, advances, and future opportunities" Journal of Magnetic Resonance Imaging, pp. 441–451, 2007.

[3] H. Kang, A. Pinti, L. Vermeiren, A. Taleb Ahmed, X. Zeng, "Tissue classification for MRI of thigh using a modified FCM method", Proceedings of the 29th Annual International Conference of the IEEE pp. 5579- 5584, 2007

[4] Huynh Van Lung, Jong-Myon Kim, "A Generalized Spatial Fuzzy C-Means Algorithm for Medical Image Segmentation", proceedings of the FUZZ-IEEE, pp. 409- 414. 2009

[5] Zhimin WANG, Qing SONG, Yeng Chai SOH and Kang SIM, "A Robust Information Fuzzy Clustering Algorithm for Medical Image Segmentation", IEEE International Conference on Granular Computing, pp. 509-514, 2010

[6] Benjamin Gillesa, Nadia Magnenat-Thalmanna, "Musculoskeletal MRI segmentation using multi-resolution simplex meshes with medial representations", Medical Image Analysis, vol. 14, pp. 291–302, 2010

[7] Pierre Dodin, Jean-Pierre Pelletier, Johanne Martel-Pelletier, and Francois Abram, " Automatic Human Knee Cartilage Segmentation From 3-D Magnetic Resonance Images", IEEE Transactions on Biomedical Engineering, vol. 57, no. 11, pp.2699-2711, November 2010

[8] Salma Essafi, G. Langs, J-F. Deux, A. Rahmouni, G. Bassez, N. Paragios, "Wavelet-driven knowledge-based mri calf muscle segmentation", IEEE International Symposium on Biomedical Imaging: From Nano to Macro, pp. 225-228, 2009.

[9] Shan Shen, William Sandham, Malcolm Granat, and Annette Sterr, " MRI Fuzzy Segmentation of Brain TissueUsing Neighborhood Attraction With Neural-Network Optimization", IEEE Transactions On Information Technology In Biomedicine, vol. 9, no. 3, pp. 459-467, Sep. 2005

[10] Tao Song, Mo M. Jamshidi, Roland R. Lee, and Mingxiong Huang, "A Modified Probabilistic Neural Network for Partial Volume Segmentation in Brain MR Image", IEEE Transactions On Neural Networks, vol. 18, no. 5, pp. 1424-1432, Sep. 2007

[11] Sufyan Y. Ababneh, Metin N. Gurcan , "An Automated Content-Based Segmentation Framework: Application to MR Images of Knee for Osteoarthritis Research", IEEE International Conference on Electro/Information Technology (EIT), pp. 1-4, 2010

[12] Xu, N. ; Bansal, R. ; Ahuja, N. , "Object Segmentation Using Graph Cuts Based Active Contours", Proceedings. 2003 IEEE Computer Society Conference on Computer Vision and Pattern Recognition, pp. 46-53, 2003.

[13] D.Jude hemanthl, D.Selvathi and J.Anitha, " "Effective Fuzzy Clustering Algorithm for Abnormal MR Brain ImageSegmentation", 2009 IEEE International Advance Computing Conference (IACC 2009)

[14] Jim X. Chen, Harry Wechsler, J. Mark Pullen, Ying Zhu, and Edward B. MacMahon "Knee Surgery Assistance: Patient Model Construction, Motion Simulation, and Biomechanical Visualization", IEEE Transactions On Biomedical Engineering, vol. 48, no. 9, pp. 1042–1052, Sep. 2001.

[15] M. Taherdangkoo, M. Yazdi, and M. H. Rezvani " Segmentation of MR Brain Images Using FCM improved by Artificial Bee Colony (ABC) Algorithm", IEEE International Conference on Information Technology and Applications in Biomedicine, pp. 1-5, 2010.

[16] J. C. Bezdek, "Pattern Recognition with Fuzzy Objective Function Algorithms," Plenum Press, New York, 1981.

[17] M. Karnan1, N. Nandha Gopal, "Hybrid Markov Random Field with Parallel Ant Colony Optimization andFuzzy C Means for MRI Brain Image segmentation", IEEE International Conference on Computational Intelligence and Computing Research, pp. 1-4, 2010.

[18] Jin Liu, Tuan D. Pham, Wei Wen, Perminder S. Sachdev, " Spatially Constrained Fuzzy Hyper-Prototype Clustering with Application to Brain Tissue Segmentation", Proc. IEEE Int. Conf. on Bioinformatics and Biomedicine, pp. 397- 400, 2010.

[19] Albert Huang, Rafeef Abugharbieh, Roger Tam, " A Hybrid Geometric–Statistical Deformable Model for Automated 3-D Segmentation in Brain MRI", IEEE Transactions On Biomedical Engineering, vol. 56, no. 7, pp. 1838-1848, July 2009.

[20] Lara C.V. Harrison, Riku Nikander, Minna Sikio, Tiina Luukkaala, Mika T. Helminen, Pertti Ryymin, Seppo Soimakallio, Hannu J. Eskola, Prasun Dastidar and Harri Sievanen, "MRI Texture Analysis of Femoral Neck: Detection of Exercise Load-Associated Differences in Trabecular Bone", Journal Of Magnetic Resonance Imaging vol. 34, pp.1359–1366, 2011.

[21] Christopher M. Larson, " Pincer-Type Femoroacetabular Impingement", Operative Techniques in Sports Medicine, vol. 20, pp. 273-280, 2012.